

INFLUENCE OF INTERACTION BETWEEN LOW AND MIDDLE LATITUDES ON ENSO VARIABILITY IN THE CANE-ZEBIAK MODEL*

Ni Yunqi (倪允琪)

Department of Atmospheric Sciences, Nanjing University, Nanjing 210093

Received May 3, 1995; revised November 14, 1995

ABSTRACT

In this paper, an error source in the atmospheric component of the CZ (Cane-Zebiak) model is discussed, which is missing a free mode in "the exact solutions". However, the improved scheme is proposed, which is the computational scheme with adjusted wind or observed u and v as lateral boundaries. The simulations show that the simulated surface wind by the improved scheme strongly bears resemblance to the observation except for the area near the west and the east boundaries of the integrated area. These results support the conclusion that the wind stress simulated by the improved scheme with lateral boundaries is much better than that simulated by the CZ model, and show that interaction between low and middle latitudes has an important influence on the ENSO variability in the CZ model. Therefore, considering its impact on the CZ model can improve capability of the CZ model for simulating ENSO variability.

Key words: interaction, ENSO variability, error source, atmospheric component, lateral boundary

I. INTRODUCTION

During the past decades, researches have led to an understanding that formation of El Niño-Southern Oscillation (ENSO) is due to the operation of a natural coupled oscillator of the ocean-atmosphere system in the tropical Pacific (Graham and White 1988; Hirst 1986; 1988; Philander et al. 1984; Cane and Zebiak 1985; Zebiak and Cane 1987). There are three main components in the ocean-atmosphere system of the tropical Pacific, that is, sea surface temperature, surface wind, and the thickness of the warm upper layer of the ocean. Among them, the importance of surface wind recently has been underscored by developments in the theory and modeling of tropical ocean-atmosphere interaction. Especially, the zonal component of the surface wind within the equatorial waveguide region becomes more important, in which its change causes changes in the slope of the sea surface and in thickness of the upper layer, finally, it can give rise to generating Kelvin waves with positive feedback process (Schopf and Suarez 1988; Battisti 1988). Away from the equator, the wind stress can cause changes in upper layer thickness via Ekman pumping process resulting in generating the baroclinic Rossby waves with the negative feedback process (Schopf and Suarez 1988; Battisti 1988; Graham 1987; Cane 1984). Obviously, these two feedback processes are necessary for formation of the ENSO cycle (Graham and

* This study was supported by the project "Study for Climate Dynamics and Climate Prediction Theory".

White 1988). Therefore, simulation of surface wind in the tropical Pacific is so important that it determines whether the ENSO cycle can be simulated in the model. Furthermore, the above studies on formation theory and dynamics of ENSO show that simple models of the atmosphere coupled with simple models of the ocean have received a great deal of achievement and attention recently. Such models have shown themselves capable of realistically reproducing the major large-scale features of the ENSO phenomena (Cane and Zebiak 1985; Zebiak and Cane 1987) and the Cane-Zebiak (CZ hereinafter) model have given successful prediction for the 1986–1987 El Nino 9 months in advance (Cane et al. 1986; Zebiak and Cane 1987). It is noted that experimental predictions with the historical data from 1960 to the present have also shown that the CZ model has the potential to produce generally reliable El Nino forecast at lead time up to a year or more (Cane et al. 1986). However, Goswami and Shukla (1991) and Blumenthal (1992) studied the predictability of the CZ model. Goswami and Shukla pointed out that the error grew up quickly after the CZ model was integrated for three months and the error mainly came from the atmospheric component of the CZ model. However, influence of interaction between low and middle latitudes on ENSO variability in the CZ model has not been considered (Cane and Zebiak 1985; Zebiak and Cane 1987). Therefore, considering the influence of interaction between low and middle latitudes in the CZ model should be important for further studying the formation mechanism of ENSO cycle. Thus, improvement of the simple atmospheric model will benefit further efforts to improve the prediction of El Nino and to develop theoretical study of ENSO using the CZ model. Apparently, there are two questions that might be still open, that is, (i) what is the major source of the errors in the atmospheric component of the CZ model; and (ii) how to improve the simple atmospheric model and better simulate the surface wind in the tropical Pacific.

In this paper, we attempt to answer the above two questions. Studying shows that there indeed exists the drawback in the simple atmospheric model resulting in major errors of the simulated surface wind. These results will be discussed in Section III. In Section IV an improved computational scheme of the simple atmospheric model will be proposed and tested, that is, to solve a complete boundary value problem with the forcing term in the tropical Pacific region using surface wind as lateral boundaries. In Section V, we discuss variability of surface wind simulated by the improved scheme. The final section is discussion and conclusions.

II. "EXACT SOLUTIONS" OF THE ATMOSPHERIC COMPONENT OF THE CZ MODEL — APPLICATION OF ADJUSTED SURFACE WIND THEORY

McCreary et al. (1991) pointed out that it is generally difficult or impossible to compare the simple model closely with observations, and hence many of them are untestable. In order to gain an insight into the error source in the simple model, however, we must look for exact solutions of the model, which not only satisfy the equations constructing the simple model, but also are close to observations. The adjusted surface wind theory proposed by Zebiak (1990), which estimates the surface pressure field using the observed winds, and then reconstructs the wind from the pressure in accordance with the governing equations, might be consistent with the above requirements.

The linear non-dimensional momentum equations may be written as

$$\epsilon u - \gamma v = -p_x, \quad (1a)$$

$$\epsilon v + \gamma u = -p_y, \quad (1b)$$

where p is the surface pressure, assuming u and v respectively to denote components of observed wind, therefore, p_x and p_y can be obtained from (1a) and (1b). But Eqs. (1a) and (1b) imply a particular relation between the wind components that does not hold in the data due to errors and neglected terms. Thus, the pressure field is not uniquely determined. The approach was to compute many estimates of the pressure field by integrated (1a–1b) along different paths and to average them. Finally, the pressure field was obtained. We use p' to denote this pressure field derived from observed wind. Then, we assume again that the wind field responding to the pressure field p' still satisfies the following equations:

$$\epsilon u' - \gamma v' = -p'_x, \quad (2a)$$

$$\epsilon v' + \gamma u' = -p'_y. \quad (2b)$$

Thus, u' and v' can be calculated from Eqs. (2a) and (2b), which refer to as adjusted wind. Furthermore, the forcing term—the heating field can be computed from the adjusted wind u' and v' and pressure p' according to the following equation (Zebiak 1990):

$$Q' = \epsilon p' + \nabla \cdot \mathbf{v}'. \quad (3)$$

It is noted that the calculated area of the heating field is one smaller circle than that of the adjusted wind and pressure. Therefore, Eqs. (2a), (2b) and (3) can reconstruct the following equations with lateral boundary conditions:

$$\epsilon u - \gamma v + p_x = 0, \quad (4a)$$

$$\epsilon v + \gamma u + p_y = 0, \quad (4b)$$

$$\epsilon p + \nabla \cdot \mathbf{v} = Q, \quad (4c)$$

$$\left. \begin{array}{l} u \\ v \\ p \end{array} \right|_{\text{lateral boundaries}} \quad (4d)$$

Here, note that u , v , p at lateral boundaries are given by the adjusted wind and pressure derived from observed wind outside the calculated area of the heating field. Obviously, “exact solutions” satisfying Eqs. (4a) – (4c) with the forcing term calculated by (3) are adjusted wind and pressure derived from the observed wind in the same area as Q term. Results (Zebiak 1990) show that adjusted wind and derived pressure are very close to observed surface wind and sea level pressure.

According to the linear theory, in fact, solution of Eq. (4) is single baroclinic mode which can be decomposed into the free mode and the forcing mode and they respectively satisfy the following equations:

$$\begin{cases} \epsilon u_1 - \gamma v_1 + p_{1x} = 0, \\ \epsilon v_1 + \gamma u_1 + p_{1y} = 0, \\ \epsilon p_1 + \nabla \cdot \mathbf{v}_1 = 0, \\ u_1, v_1, p_1 |_{\text{lateral boundary}} \neq 0, \end{cases} \quad (5)$$

where the free mode is satisfied, and

$$\begin{cases} \epsilon u_2 - y v_2 + p_{2x} = 0, \\ \epsilon v_2 + y u_2 + p_{2y} = 0, \\ \epsilon p_2 + \nabla \cdot \mathbf{v}_2 = Q, \\ u_2, v_2, p_2 |_{\text{lateral boundary}} = 0, \end{cases} \quad (6)$$

where the forcing mode is satisfied. Obviously, solutions of Eq. (5) plus solutions of Eq. (6) construct solutions of Eq. (4), which are "exact solutions" of atmospheric component of the CZ model with the forcing term Q calculated by Eq. (3).

III. DIFFERENCE BETWEEN THE SOLUTION OF THE ATMOSPHERIC COMPONENT OF THE CZ MODEL AND THE "EXACT SOLUTION"

In the original computational scheme of the atmospheric component of the CZ model, Eq. (4) is solved by using spectral decomposition in x , and finite differencing in y . Therefore, the finite difference equation of solving the spectral coefficient V may be written as

$$\begin{aligned} V_{j-1} + \left(\frac{i\pi\Delta y^2 k}{2\epsilon} - 2 - \frac{\Delta y^2}{4} y_j^2 - \Delta y^2 (\epsilon^2 + k^2) \right) V_j + V_{j+1} \\ = - \frac{\Delta y}{2} \tilde{Q}_{j-1} + \frac{i\pi\Delta y^2 k}{2\epsilon} y_j \tilde{Q}_j + \frac{\Delta y}{2} \tilde{Q}_{j+1}, \quad j = 1, N \end{aligned} \quad (7)$$

where Δy is the grid spacing, and N is the total number of interior grid point in y . The boundary condition in (7) is that $V=0$ (i. e. $V_0=0$ and $V_{N+1}=0$) at the pole. At same time, $\tilde{Q}_0=0$ and $\tilde{Q}_{N+1}=0$ are given.

Once the $\{V_j\}$ are found, the $\{U_j\}$ are obtained using

$$(k^2 + \epsilon^2) U_j = \epsilon y_j V_j / 2 + \frac{ik}{2\Delta y} (V_{j+1} - V_{j-1}) + ik \tilde{Q}_j, \quad j = 1, N. \quad (8)$$

In this calculation, the domain in y is from -7.9 (79°S) to $+7.9$ (79°N), and $\Delta y = 0.2$ (-200 km). The spectral decomposition is done using a 64-point FFT, and the domain in x is the full 360° longitude, giving a spatial resolution (in x) of about 600 km. It is noteworthy that parameterized method for the convective heating, which is related to SSTA, convergence in the lower troposphere, and feedback to surface wind, is utilized in the atmospheric component of the CZ model. However, these feedback processes between latent heat release in areas of organized convection and the wind field are available for the tropical region. In order to compare the solutions of Eqs. (7) and (8) with adjusted wind ("exact solutions"), Q calculated by (3) is used instead of parameterized Q in (7) and (8) from 25°S to 25°N .

The difference maps between the simulated surface wind by (7), (8) and (3) and adjusted wind are shown in Figs. 1a–1f. The difference maps clearly show that there exist obvious differences in the simulated surface winds by (7) and (8), especially off the equator, and the differences are decayed far away from the north and south boundaries of the area where Q is calculated by (3). Furthermore, the differences still have an influence on the wind along the equator in the most cases although the differences near the equator are much smaller than those north of 5°N or south of 5°S .

Where do the differences come from?

At first, we have to keep in mind that (i) the heating field Q is only calculated in the Pacific region from 25°S to 25°N by using Eq. (3) from adjusted wind and derived pressure

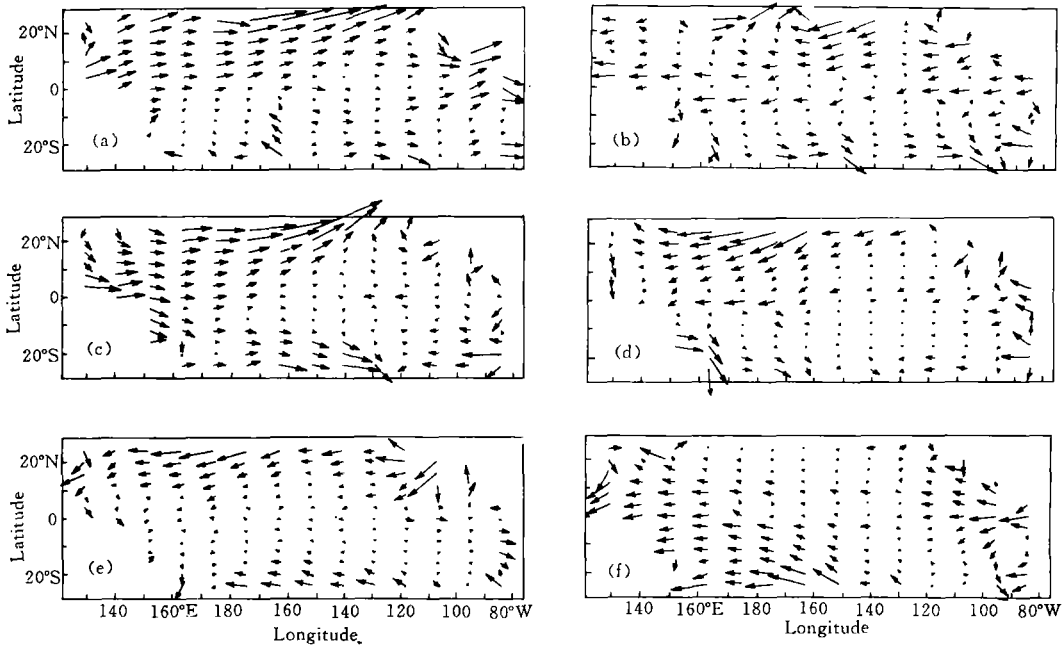


Fig. 1. Difference maps between the simulated surface wind anomalies by the CZ model and adjusted wind anomalies. (a) March 1983; (b) January 1984; (c) February 1986; (d) January 1987; (e) December 1987; (f) July 1988.

and Q is zero outside the region; (ii) the model is integrated from 0° to 360° in longitude and from 79°S to 79°N in latitude with the lateral boundary condition $v=0$. Thus, the solutions in the area with non-zero Q can be obtained and the solutions along the circle outside the area with non-zero Q (at 27°S and 27°N) are only determined by v and Q along the circle of the boundary of the area with non-zero Q , which are not related to u and v outside the area with non-zero Q , and the solutions in other area are equal to zero by using Eqs. (7) and (8).

Therefore, it can be thought that the atmospheric component of the CZ model written by Eqs. (7) and (8) with the calculated domain from 0° to 360° in longitude and from 79°S to 79°N in latitude and Q given in the tropical Pacific from 27°S to 27°N (including non-zero Q from 25°S to 25°N and zero Q along the 27°S and 27°N latitudes) and zero Q in other areas is basically equivalent to the following boundary value problem:

$$\begin{cases} \epsilon u - yv + p_x = 0, \\ \epsilon v + yu + p_y = 0, \\ \epsilon p + \nabla \cdot \mathbf{v} = Q, \\ u, v, p|_{\text{lateral boundary}} = 0, \quad \text{at } y = 2.9, -2.9 \end{cases} \quad (9)$$

and the calculated area covers the tropical Pacific from 27°S to 27°N . Comparing (9) with (5), (6) and (4), we can find that (9) is responding to (6), that is, the solutions of (9) are only involving the forcing mode of Eq. (4) which produces "exact solutions" of atmospheric component of the CZ model. Obviously, the "exact solutions" of Eq. (4) subtracting the solutions of Eq. (9) should be equal to the free mode from Eq. (5). Thus, it is clearly that the solutions from the original schemes (7) and (8) of the atmospheric

component of the CZ model lost the free mode part of the "exact solutions". The free mode implies impact of lateral boundaries with non-zero on the solutions inside the calculated area. This means that in the original computational scheme, interaction between flow fields outside and inside the calculated area is not involved. As a result, the solutions from this scheme only can express the flow field in an isolated tropical atmospheric system. Therefore, we can conclude that the source of the errors in the original scheme of atmospheric component of the CZ model comes from loss of the free mode included in the "exact solutions". In other words, the effect of the flow field outside the calculated area on that inside the area unconsidered in the scheme is a source causing the differences between the solutions from the atmospheric component of the CZ model and "the exact solutions".

IV. AN IMPROVED SCHEME WITH COMPLETE LATERAL BOUNDARY CONDITION

The scheme exactly solving Eq. (4) should involve two aspects: one is that the computational scheme includes complete boundary conditions, which is proposed as complete boundary value problem; the other is that the solutions from the scheme completely include free mode and forcing mode of Eq. (4). Therefore, an improved scheme which satisfies the above requirements should be as follows.

As same as the original scheme of the atmospheric component of the CZ model, Eq. (4) is solved by using spectral decomposition in x and finite differencing in y . Therefore, the following equations can be obtained:

$$\begin{cases} \epsilon U - yV/2 = ikP, & (10a) \\ \epsilon V + yU/2 = -P_y, & (10b) \\ \epsilon P + ikU + V_y = -\tilde{Q}, & (10c) \end{cases}$$

where U , V , P , \tilde{Q} are spectral coefficients. From Eqs. (10a) and (10c), we can get the following formula:

$$U(\epsilon^2 + k^2) = ik\tilde{Q} + y\epsilon V/2 + ikV_y. \quad (11)$$

Similarly, the following equation is obtained from Eqs. (10a) and (10b):

$$\epsilon U_y - ik_y U/2 - ik\epsilon V - V/2 - \frac{y}{2}V_y = 0, \quad (12)$$

and from Eqs. (10b) and (10c), we can obtain

$$ikU_y + V_{yy} - \epsilon^2 V - \epsilon yU/2 = -\tilde{Q}_y. \quad (13)$$

Eliminating the first term in Eqs. (12) and (13), and substituting (11) into the resulting equation, the variable U is finally eliminated and the following equation with a variable V is obtained:

$$V_{yy} + \left(-\frac{y^2}{4} + \frac{ik}{2\epsilon} - \epsilon^2 - k^2\right)V = -\tilde{Q}_y + \frac{ik}{2\epsilon}y\tilde{Q}_y. \quad (14)$$

Eliminating the V_{yy} term in (13) using (12) and then substituting (11) into the resulting equation, the variable V is eliminated and we can obtain the equation with a variable U as follows:

$$U_{yy} - \left(\frac{y^2}{4} + \frac{ik}{2\epsilon} + \epsilon^2 + k^2\right)U = -ik\tilde{Q} + \frac{1}{\epsilon}V_y - \frac{y}{2\epsilon}\tilde{Q}_y. \quad (15)$$

Assuming

$$\begin{aligned} U_{yy} &= \frac{U_{j+1} + U_{j-1} - 2U_j}{\Delta y^2}, \\ V_{yy} &= \frac{V_{j+1} + V_{j-1} - 2V_j}{\Delta y^2}, \\ V_y &= \frac{V_{j+1} - V_{j-1}}{2\Delta y}, \\ \tilde{Q}_y &= \frac{\tilde{Q}_{j+1} - \tilde{Q}_{j-1}}{2\Delta y}, \end{aligned}$$

the finite difference Eqs. (14) and (15) may be written as

$$\begin{aligned} &V_{j-1} + \left(\frac{i\pi\Delta y^2 k}{2\epsilon} - 2 - \frac{\Delta y^2}{4} y_j^2 - \Delta y^2 (\epsilon^2 + k^2) \right) V_j + V_{j+1} \\ &= -\frac{\Delta y}{2} Q_{j-1} + \frac{i\pi\Delta y^2 k}{2\epsilon} y_j Q_j + \frac{\Delta y}{2} Q_{j+1}, \quad j = 1, N, \end{aligned} \quad (16)$$

$$\begin{aligned} &U_{j-1} - \left(\frac{i\pi\Delta y^2 k}{2\epsilon} + 2 + \frac{\Delta y^2}{4} y_j^2 + \Delta y^2 (\epsilon^2 + k^2) \right) U_j + U_{j+1} \\ &= -\frac{\Delta y}{2\epsilon} (V_{j+1} - V_{j-1}) + \frac{\Delta y}{4\epsilon} y_j (Q_{j+1} - Q_{j-1}) - i\pi\Delta y^2 k Q_j, \quad j = 1, N \end{aligned} \quad (17)$$

and the lateral boundary conditions are

$$\begin{matrix} U \\ V \end{matrix} \Big|_{j=0, N+1}. \quad (18)$$

The difference Eqs. (16) and (17) with the forcing term \tilde{Q} calculated by (3) are calculated from 0° to 360° in longitude and from 25°N to 25°S in latitude. The lateral boundary conditions are given by U component and V component of the adjusted wind at 27°N and 27°S . In order to correctly compute \tilde{Q}_y in Eqs. (14) and (15) at 25°N and 25°S , the \tilde{Q} values at 27°N and at 27°S are also given using (3).

The same six cases as those calculated by the original scheme of atmospheric component, which are arbitrarily choose, are calculated by (16), (17) and (18). The simulated surface wind and difference between simulated surface wind and adjusted wind are respectively given in Figs. 2–7.

Figures 2–7 clearly show that the improved computational schemes (16) and (17) with lateral boundary condition (18) simulate the adjusted wind very well except for those near the west and east boundaries of the area where Q is calculated by (3). Especially, it is noteworthy that the differences in the area from 160°E to 120°W are generally smaller than 1.0, and even they do not have any significant influence on the simulated zonal wind along the equator from 160°E to 120°W . Apparently, the results from (16)–(18) are much better than those from (7) and (8). Why are there still marked differences near the west and east boundaries of the area where Q is calculated by (3)? This is because the Q field is only given in the Pacific region from 27°N to 27°S and from 129.375°E to 73.125°W and discontinuity of the Q field along the latitudinal zone appears at the west and east side boundaries of the non-zero Q area. As a consequence, there exist apparent differences in \tilde{Q} near the west and east boundaries of the non-zero Q area when Q is spectrally expanded

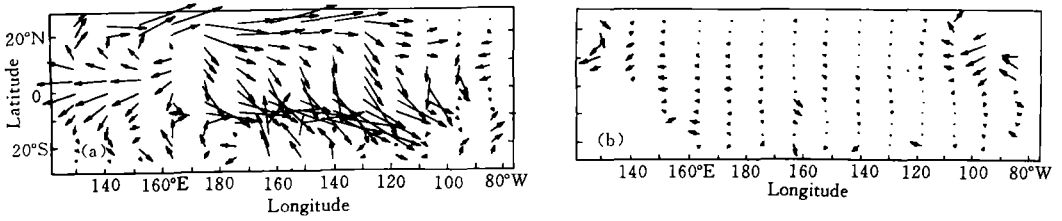


Fig. 2. (a) the simulated surface wind anomalies in March 1983 by version of the CZ model: (b) the difference map between simulated surface wind anomalies and adjusted wind anomalies in March 1983.

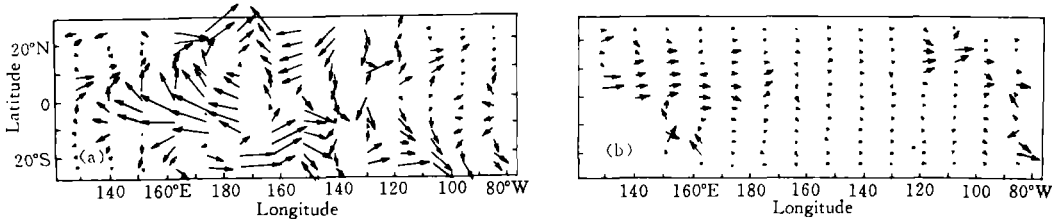


Fig. 3. As in Fig. 2. except for January 1984.

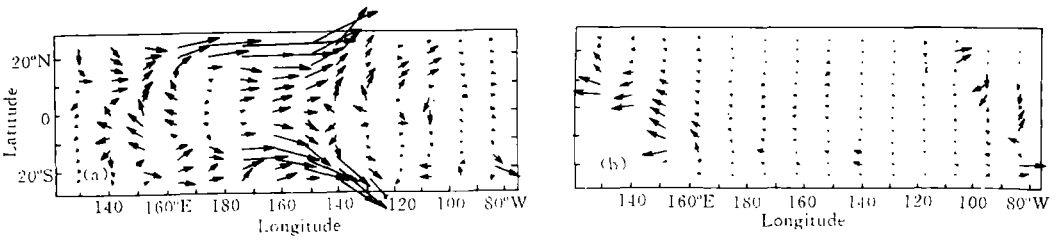


Fig. 4. As in Fig. 2. except for February 1986.

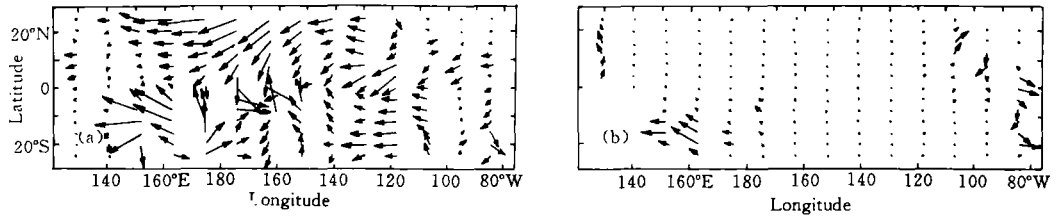


Fig. 5. As in Fig. 2. except for January 1987.

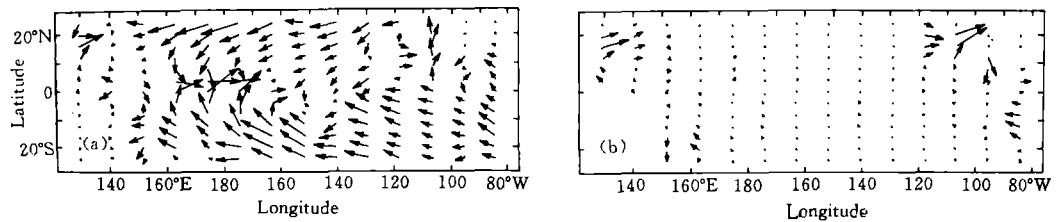


Fig. 6. As in Fig. 2. except for December 1987.

along the latitudinal circle, and errors of simulated surface wind can be arisen from errors of \tilde{Q} . Obviously, it also reflects that schemes (16) – (18) still do not consider the

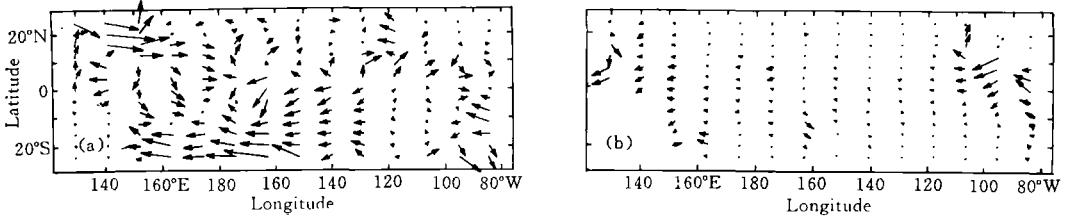


Fig. 7. As in Fig. 2. except for July 1988.

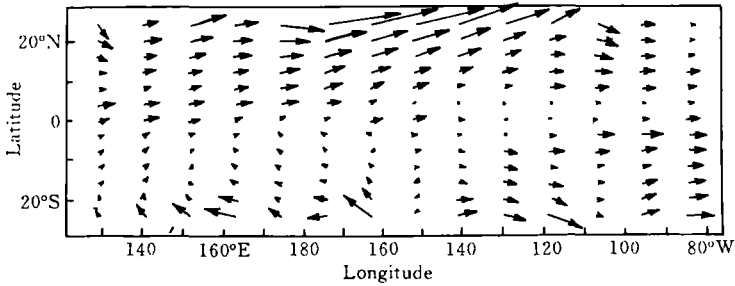


Fig. 8. Difference map between the simulated surface wind anomalies by version of the CZ model and those by the CZ model in March 1982.

influence of flow field outside the west and east boundaries of non-zero Q area on the flow field of the interior region, and the influence of flow field outside the north and south boundaries of the non-zero Q area on the flow field of the interior region is only considered.

It is noteworthy that the simulated surface wind in March 1983 (see Fig. 2a) bears a strong resemblance to that in observation, in which the westerly anomalies to the west of 170°E dominate from 20°S to 20°N and the easterly anomalies to the east of 170°E from 20°S to 20°N . The difference between both surface winds is small except for the area near the west and east boundaries of the non-zero Q area (Fig. 2b). Figure 3b shows that the easterly anomalies to the west of 170°E are strengthened and the westerly anomalies to the west of 170°E are weakened although the strengthened and weakened values are less than 1.0 from 140°E to 110°W , especially along the equator. Figure 8 represents the difference between the surface wind from the improved scheme and the CZ model in March 1983. It is clearly shown that the westerly anomalies to the east of 170°E are weakened, especially north of 10°N , and the easterly anomalies to the west of 170°E are strengthened in the CZ model. Fortunately, the differences along the equator between the improved scheme and the CZ model are less than 1.0. The above result indicates that the improved scheme is able to improve the simulation during the El Nino events compared with the CZ model.

Figures 9 and 10 respectively give difference of surface wind between the improved scheme and the CZ model in Feb. 1986 and Jan. 1984. Figures 9 and 10 clearly show that the simulated surface wind has been improved a lot by the improved scheme and it is interesting that the difference surface winds shown in Figs. 9 and 10 are very similar to those in Figs. 1a and 1b. This fact further confirms that the error source of the CZ model is due to unconsidering the impact of surface wind outside the calculated area by (3) on that in the interior area, which means that the CZ model lost the free mode of Eq. (4) regardless of

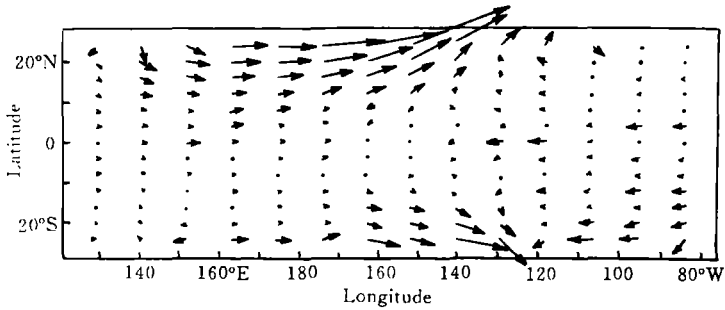


Fig. 9. As in Fig. 8. except for February 1986.

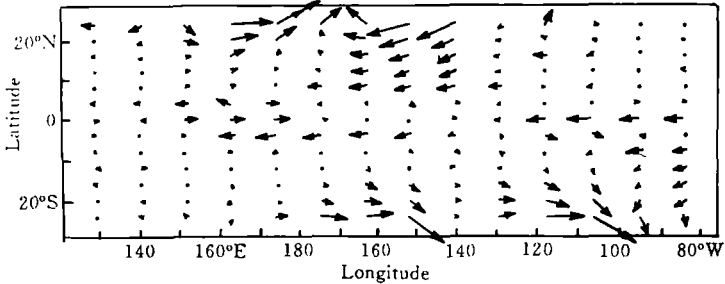


Fig. 10. As in Fig. 8. except for January 1984.

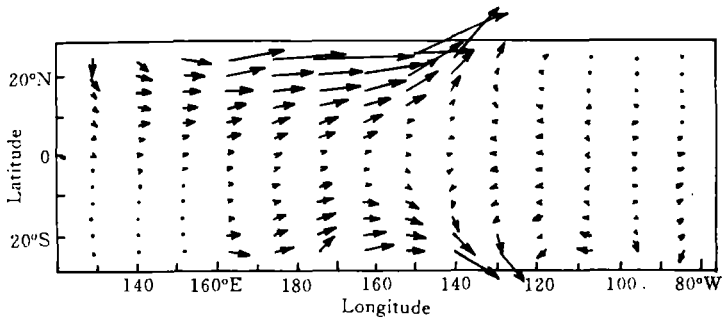


Fig. 11. Impact of lateral boundaries on surface wind anomalies in the interior area in February 1986.

the errors resulting from the parameterized heating field.

In order to further verify the above fact, the solutions with free mode are solved by using (16) and (17) with non-zero lateral boundary conditions and zero Q in the whole interior area. Figure 11 gives a pure impact of north and south boundaries on solutions in the interior area. Comparing Fig. 11 with Fig. 9 and Fig. 1a, the surface wind anomalies resulting from the north and south boundaries in Fig. 11 are well consistent with the difference surface winds in Fig. 9 and Fig. 1a. This result completely proves this fact that losing a free mode in the CZ model is the main error source of the CZ model regardless of the errors from the parameterized heating field.

V. APPLICATION OF THE IMPROVED SCHEMES TO ATMOSPHERIC COMPONENT OF THE CZ MODEL

The atmospheric component is from Jan. 1970 to Dec. 1989. The correlation coefficients between simulated wind stress in the CZ model and observed wind stress from FSU

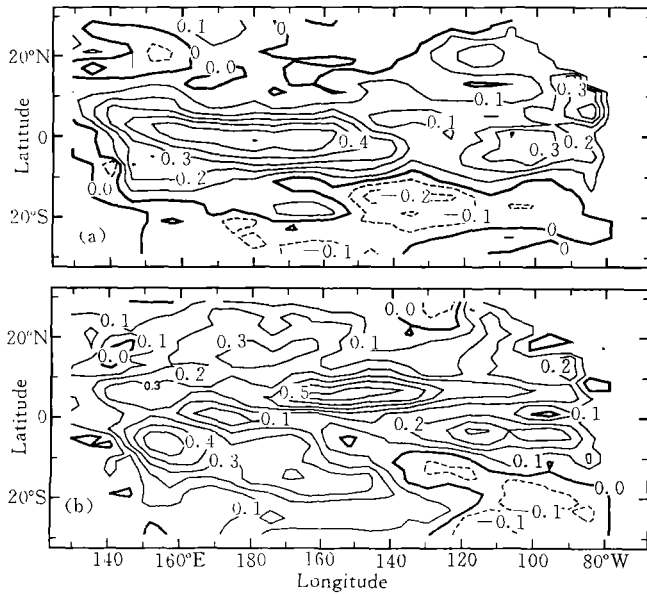


Fig. 12. Correlation between wind stress anomalies in the CZ model and observation. (a) x component; (b) y component.

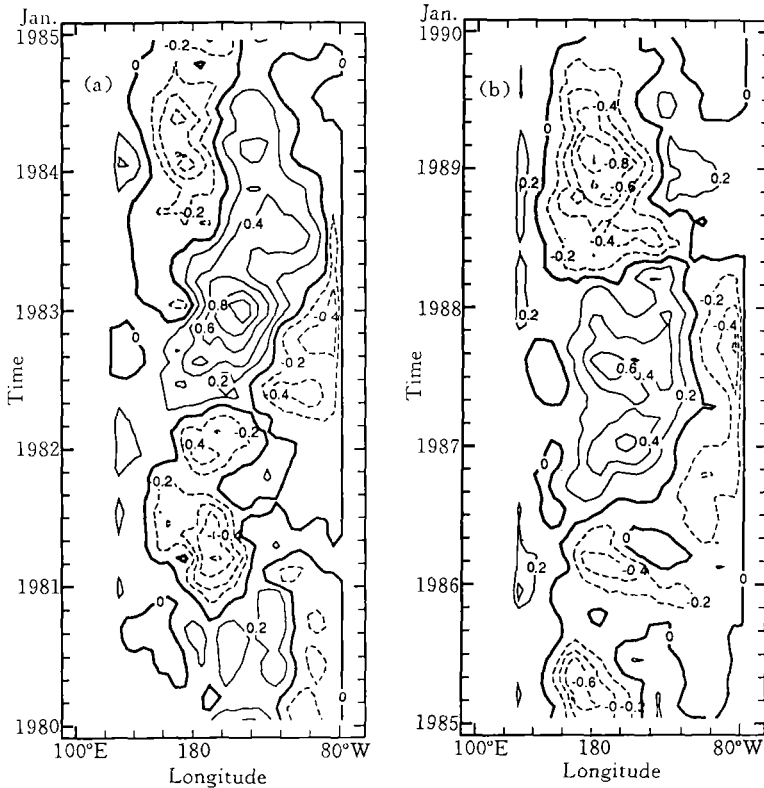


Fig. 13. Time-longitude cross section of wind stress anomalies along the equator in the CZ model. (a) x component; (b) y component.

are shown in Fig. 12. The correlation map shows that the areas where the coefficients are greater than 0.5 in the u component is located from 4°S to 4°N and from 155°E to 155°W

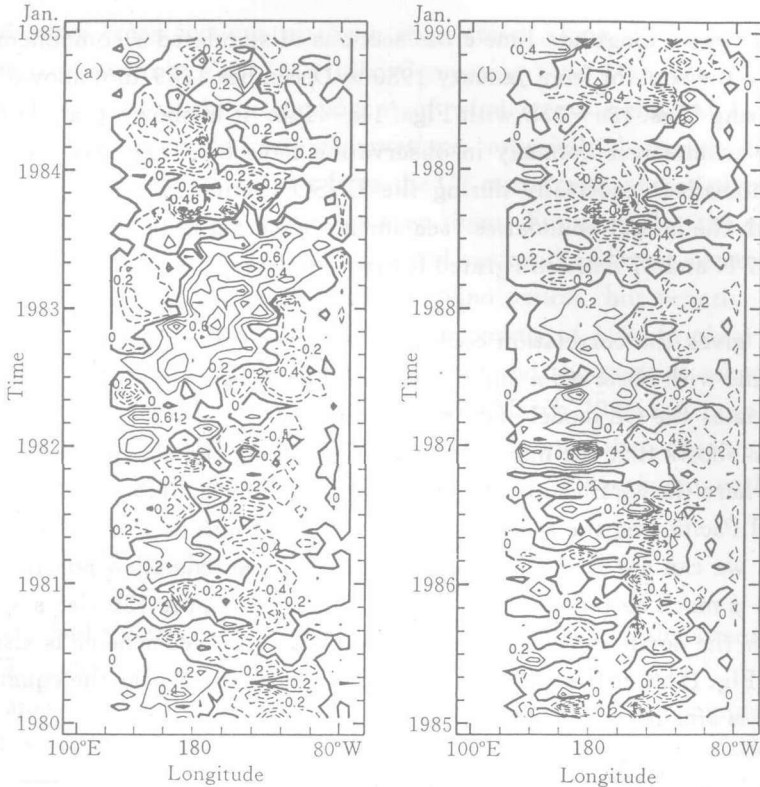


Fig. 14. As in Fig. 13. except for observation.

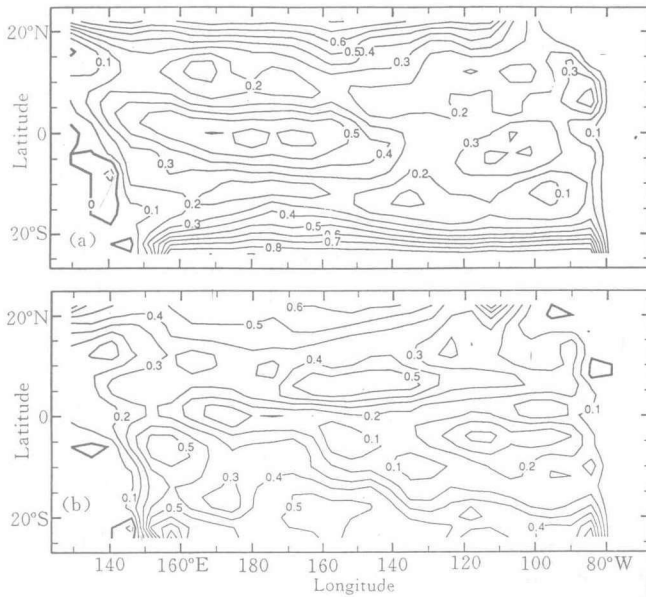


Fig. 15. As in Fig. 12. except for version of the CZ model.

and in the v component located from 3°N to 9°N and from 170°W to 130°W and near Australia. These features have captured the main characteristics of wind stress near the equator, which control formation and evolution of the ENSO events (Cane et al. 1986).

Figures 13a–13b give longitude-time cross sections of simulated x component wind stress anomalies along the equator from January 1980 to December 1989 (not shown from 1970 to 1979). Comparing Figs. 13a–13b with Figs. 14a–14b, it is shown that the main characteristics of the wind stress anomaly in observation have been captured by the simulated wind stress anomalies, especially during the ENSO events. The improved atmospheric component with the lateral boundaries, sea surface wind anomalies or sea surface pressure anomalies at 27°N and 27°S are integrated for twenty years from January 1970 to December 1989.

Figure 15 gives the correlation coefficients between wind stress u simulated by the improved scheme with observed u and v as lateral boundaries and Q calculated by the same parameterization as the CZ model and observation.

Figure 15a shows that the maximum coefficient along the equator reaches to over 0.6 and the area where the coefficients are greater than 0.5 have almost occupied western and central tropical Pacific and the areas north of 15°N and south of 15°S . Comparing Fig. 15a with Fig. 12a, we can see that the u component of the simulated wind stress by the improved scheme is much better than that by the CZ model. Figure 15b also shows that the v component near the north and south boundaries in the improved scheme is also better than that shown in Fig. 12b but the maximum correlation coefficient near the equator in the improved scheme is smaller than that in the CZ model.

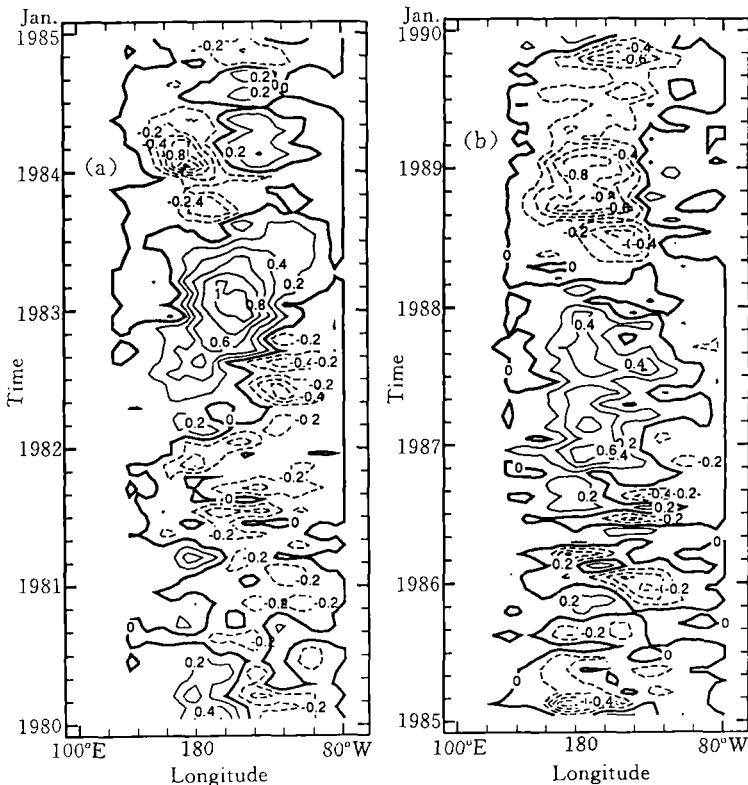


Fig. 16. As in Fig. 13, except for version of the CZ model.

Longitude-time cross sections of the u wind stress along the equator from the improved scheme are shown in Figs. 16a–16b. Comparing Figs. 16a–16b with observations shown in Figs. 14a–14b, the u component of wind stress simulated by the improved scheme strongly bears resemblance to observations, especially during the El Niño and La Niña events. If we compare the results from the CZ model with observations in detail, we can find that there are some differences between them. For example, the positive anomalies of the u wind stress over the equatorial central-eastern Pacific are successfully simulated by the CZ model during the 1982–1983 El Niño period, but negative anomalies are appearing in this area from September 1983 to beginning of 1984 in observations; while positive anomalies are still keeping in the CZ model and the positive anomalies over the equatorial central-eastern Pacific from July 1986 to March 1988 and negative anomalies from March 1988 to end of 1989 in the CZ model are stronger than observations. However, the simulated u wind stress in the improved scheme is consistent with observations well.

VI. DISCUSSION AND CONCLUSIONS

The above results clearly show that there is an error source in the atmospheric component of the CZ model, which is missing a free mode in the solutions.

In this paper, the improved scheme is proposed, which is the computational scheme with adjusted wind or observed u and v as lateral boundaries. The simulations show that the simulated surface wind by the improved scheme strongly bears resemblance to the observation except for the area near the west and the east boundaries of the integrated area. The difference between surface winds simulated by the improved schemes and by the CZ model just is the free mode of the exact solutions of the model equations with adjusted wind as lateral boundaries.

The improved scheme is applied to the atmospheric component with the Q calculated by a parameterization with a feedback process. The correlation coefficients between wind stress simulated by the improved scheme and observation are higher than those between wind stress simulated by the CZ model and observations. It is noteworthy that the correlation coefficients of the u component near the equator are higher in the improved scheme than those in the CZ model. It has been pointed out that the zonal component of the surface wind within the equatorial waveguide region is more important because its change is directly related to ENSO variability (Schopf and Suarez 1988; Battisti 1988). Therefore, these results clearly reflect that the impact of lateral boundaries on the simulated u component is significant even if the area is located near the equator but the impact of lateral boundaries on the simulated v component near the equator is not significant. The longitude-time cross sections of the u component and v component of the wind stress simulated by improved scheme with the same Q as in the CZ model are more consistent with the observed than those from simulated wind stress by the CZ model. These results support the conclusion that the wind stress simulated by the improved scheme with lateral boundaries are much better than those simulated by the CZ model. Obviously, adjusted wind procedure (Zebiak 1991) looks like a filter which makes surface wind, sea level pressure and forcing term satisfy the model equations. The observed surface wind or sea level pressure

has to be filtered by this procedure before they are used as lateral boundaries.

However, the above scheme with adjusted wind or observed wind as lateral boundaries only can be used to simulate the surface wind stress in the tropical ocean because the lateral boundaries come from observations. If the scheme with lateral boundaries is applied to the prediction model, apparently, the lateral boundaries with surface wind have to be predicted.

On the whole, interaction between the low and the middle latitudes has an important influence on the ENSO variability in the CZ model. Therefore, considering its impact on the CZ model can improve capability of the CZ model for simulating ENSO variability.

I would like to express thanks for support and discussion from Dr. S. E. Zebiak and Prof. Mark A. Cane, Lamont-Doherty Earth Observatory of Columbia University.

REFERENCES

- Battisti, D. S. (1988). Dynamics and thermodynamics of a warming event in a coupled tropical atmosphere-ocean model. *J. Atmos. Sci.*, **45**: 2889–2919.
- Blumenthal, M. B. (1991). Predictability of a coupled ocean-atmosphere model. *J. Clim.*, **4**: 766–784.
- Cane, M. A. and Patton, R. J. (1984). A numerical model for low frequency equatorial dynamics. *J. Phys. Oceanogr.*, **14**: 1853–1863.
- Cane, M. A. and Zebiak, S. E. (1985). A theory for El Nino and the Southern Oscillation. *Science*, **228**: 1085–1087.
- Cane, M. A., Zebiak, S. E. and Dolan, S. C. (1986). Experimental forecasts of El Nino. *Nature*, **321**: 827–832.
- Graham, N. E. and Barnett, T. P. (1987). Sea surface temperature, surface wind divergence, and convection over tropical ocean. *Science*, **238**: 657–659.
- Graham, N. E. and White, W. B. (1988). The El Nino cycle: A natural oscillator of the Pacific ocean-atmosphere system. *Science*, 1293–1302.
- Goswami, B. N. and Shukla, J. (1991). Predictability of a coupled ocean-atmosphere model. *J. Clim.*, **4**: 3–22.
- Hirst, A. C. (1986). Unstable and damped equatorial modes in simple coupled ocean-atmosphere models. *J. Atmos. Sci.*, **43**: 606–630.
- Hirst, A. C. (1988). Slow instabilities in tropical ocean basin-global atmosphere models. *J. Atmos. Sci.*, **45**: 830–852.
- McCreary, J. P., Jr. and Anderson, D. L. T. (1991). An overview of coupled ocean-atmosphere models of El Nino and the Southern Oscillation. *J. Geophys. Res.*, **96**: 3125–3150.
- Philander, S. G. H., Yamagata, T. and Pacanowski, R. C. (1984). Unstable air-sea interactions in the tropics. *J. Atmos. Sci.*, **41**: 604–613.
- Schopf, P. S. and Suarez, M. J. (1988). Vacillations in a coupled atmosphere-ocean model. *J. Atmos. Sci.*, **45**: 549–566.
- Zebiak, S. E. and Cane, M. (1987). A model El Nino/Southern Oscillation. *Mon. Wea. Rev.*, **115**: 2262–2278.
- Zebiak, S. E. (1990). Diagnostic studies of Pacific surface winds. *J. Clim.*, **3**: 1016–1031.